

BRIEF REPORT



## Tumors exploit CXCR4<sup>hi</sup>CD62L<sup>lo</sup> aged neutrophils to facilitate metastatic spread

Zhenzi Peng<sup>a</sup>, Cuiwei Liu<sup>a,b,c</sup>, Aaron R. Victor<sup>c</sup>, Duo-Yao Cao<sup>a</sup>, Luciana C. Veiras<sup>a</sup>, Ellen A. Bernstein<sup>a</sup>, Zakir Khan<sup>a,d,c</sup>, Jorge F. Giani<sup>a,d</sup>, Xiaojiang Cui<sup>a,b</sup>, Kenneth E. Bernstein<sup>a,d</sup>, and Derick Okwan-Duodu<sup>b</sup>

<sup>a</sup>Department of Biomedical Sciences, Cedars-Sinai Medical Center, Los Angeles, CA, USA; <sup>b</sup>Department of Surgery, Cedars-Sinai Medical Center, Los Angeles, CA, USA; <sup>c</sup>Department of Pathology and Laboratory Medicine, Cedars-Sinai Medical Center, Los Angeles, CA, USA; <sup>d</sup>Cancer Center, Union Hospital, Tongji Medical College, Huazhong University of Science and Technology, Wuhan, China

### ABSTRACT

Granulocytes are key players in cancer metastasis. While tumor-induced *de novo* expansion of immunosuppressive myeloid-derived suppressor cells (MDSCs) is well-described, the fate and contribution of terminally differentiated mature neutrophils to the metastatic process remain poorly understood. Here, we show that in experimental metastatic cancer models, CXCR4<sup>hi</sup>CD62L<sup>lo</sup> aged neutrophils accumulate via disruption of neutrophil circadian homeostasis and direct stimulation of neutrophil aging mediated by angiotensin II. Compared to CXCR4<sup>lo</sup>CD62L<sup>hi</sup> naive neutrophils, aged neutrophils more robustly promote tumor migration and support metastasis through the increased release of several metastasis-promoting factors, including neutrophil extracellular traps (NETs), reactive oxygen species, vascular endothelial growth factors, and metalloproteinases (MMP-9). Adoptive transfer of aged neutrophils significantly enhanced metastasis of breast (4T1) and melanoma (B16LS9) cancer cells to the liver, and these effects were predominantly mediated by NETs. Our results highlight that in addition to modulating MDSC production, targeting aged neutrophil clearance and homeostasis may be effective in reducing cancer metastasis.

### ARTICLE HISTORY

Received 25 August 2020  
Revised 14 December 2020  
Accepted 28 December 2020

### KEYWORDS

Metastasis; aged neutrophils; neutrophil homeostasis; inflammation

### Introduction

Inflammation is critical to the metastatic process, which accounts for the majority of cancer-related deaths.<sup>1–3</sup> Tumor cells sustain inflammation by mobilizing granulocytes and other myeloid cells from the bone marrow.<sup>4,5</sup> Indeed, an increase in neutrophil-lymphocyte ratio portends an elevated risk of metastasis, a reduced overall survival, and a poor response to various forms of therapies in multiple cancer types including breast cancer and melanoma.<sup>6</sup>

The best-described source of metastasis-supporting neutrophilic inflammation is the hijacking of myeloid differentiation to generate immunosuppressive myeloid-derived suppressor cells (MDSCs).<sup>7</sup> However, not all neutrophils in the metastatic cancer environment are granulocytic MDSCs (gMDSCs). Indeed, a recent single-cell sequencing analysis of mice and humans with breast cancer revealed that gMDSCs only emerge from a distinct branch point along the developmental trajectory of neutrophils, indicating that normal mature neutrophils are also generated in the cancer environment.<sup>8</sup> The goal of our study was to determine how metastatic cancers regulate these other mature neutrophils that are not gMDSCs, and how these cells in turn impact the metastatic process. Addressing this knowledge gap is crucial, as pro- and anti-tumor mature neutrophils have been described.<sup>9,10</sup>

It is increasingly recognized that mature neutrophils in the circulation are not homogeneous.<sup>11</sup> A major source of neutrophil heterogeneity is the temporal, physiologic process whereby naive neutrophils – characterized by a CXCR4<sup>lo</sup>CD62L<sup>hi</sup>

expression profile – age through downregulation of CD62L and upregulation of CXCR4. These alterations facilitate the homing of CXCR4<sup>hi</sup>CD62L<sup>lo</sup> aged neutrophils to the bone marrow in a rhythmic circadian fashion for efferocytic clearance.<sup>12,13</sup> Aged neutrophils represent a highly inflammatory subset of neutrophils purported to enhance the immunologic defense against invading pathogens.<sup>14</sup> Their numbers are increased in gut microbiome-associated inflammatory states including sickle cell disease,<sup>13,15,16</sup> but their role in cancer biology is unknown. Moreover, how metastatic cancers affect the aged-naive neutrophil homeostasis is not described.

Here, we show that metastatic tumor-bearing mice utilize multiple mechanisms to disproportionately expand aged neutrophils. These cells enhance cancer metastasis far better than their naive counterparts. Our results reveal a previously undescribed mechanism employed by malignant tumors to provoke deleterious neutrophilic inflammation beyond MDSCs. This offers a potentially new approach to target mature neutrophil subset in cancer.

### Materials and methods

#### Animals

Eight to twelve-week-old male C57BL/6J, female Balb/C, and male green fluorescent protein (GFP) positive mice were purchased from The Jackson Laboratory. The animals were housed and cared for in agreement with guidelines approved by the Cedars-

Sinai Institutional Animal Care and Use Committee. Mice were maintained on a 12 h light/12 h dark cycle.

### Metastasis models

Intravenous injections were performed with  $1 \times 10^5$  tumor cells in 100  $\mu$ l phosphate-buffered saline (PBS). To induce liver metastasis, standard intrasplenic inoculation followed by splenectomy was performed as previously described.<sup>17</sup> A 27-gauge needle was used to inject  $1 \times 10^5$  cells in 50  $\mu$ l PBS. By performing splenectomy, this serves the dual purpose of preventing the development of large splenic tumors while also preventing the generation and accumulation of splenic MDSCs in close proximity to the liver. The extent of metastasis was analyzed by counting visible nodules on all lobes of the lung or liver after 14 d using a stereomicroscope.

### Tumor cells and culture

The highly metastatic 4T1 breast cancer cells, poorly metastatic B16F0, and its related highly metastatic B16F10 melanoma cell lines were obtained from the American Type Culture Collection (Manassas, VA).<sup>18</sup> B16LS9 melanoma cell line was originally obtained from Dr. Hans Grossniklaus (Emory University).<sup>19</sup> All cell lines were confirmed to be negative for *Mycoplasma* before culture using VenorTMGeM Mycoplasma Detection Kit (Sigma, MP0025). All cells were maintained in DMEM medium supplemented with 10% fetal bovine serum (FBS, Sigma-Aldrich, St. Louis, MO) at 37°C, 5% CO<sub>2</sub>.

For tumor-conditioned media preparations, tumor cells were incubated for 16–18 h at 37°C with 5% CO<sub>2</sub>. Upon reaching approximately 80% confluence, cell-free supernatant was collected using 0.22  $\mu$ m filters (EMD Millipore) and immediately stored at –80°C.

### Flow cytometry and FACS sorting

Samples were lysed with RBC lysis buffer, washed with FACS staining buffer (Biolegend) before incubation with an Fcy blocker (Biolegend) on ice for 10 min. Cells were stained with an antibody cocktail for 30 min on ice. Isotype-matched antibodies were used as negative controls. Multiparametric flow cytometry was performed on an LSRII (BD) and analyzed with the FlowJo software package (Tree Star). Dead cells were excluded by FSC, SSC, and DAPI-positive gating. Neutrophils were gated as CD11b<sup>+</sup>Ly6G<sup>+</sup>. Aged neutrophils were CXCR4<sup>hi</sup>CD62L<sup>lo</sup> cells within the neutrophil population, while naïve neutrophils were gated as CD62L<sup>hi</sup>CXCR4<sup>lo</sup>. Cell sorting was performed on the BD Influx Cell Sorter.

For analysis of neutrophil aging in vivo, circadian blood samples were collected every 4 h during a 24-h period from mice, starting at the first hour at the onset of light (ZT1). In the bone marrow, mature neutrophils were identified as Ly6G<sup>+</sup>CXCR2<sup>+</sup>, whereas immature neutrophils were identified as Ly6G<sup>+/lo</sup>CXCR2<sup>-20</sup>

Macrophages were identified as Gr-1<sup>lo</sup>CD115<sup>lo</sup>F4/80<sup>+</sup>SSC<sup>lo.21</sup> Natural killer (NK) cells were identified as NK1.1<sup>+</sup>CD49b<sup>+</sup>CD3<sup>-</sup>

cells. T regulatory cells were defined as FoxP3<sup>+</sup> CD25<sup>+</sup> cells within the CD4<sup>+</sup> gated lymphocytes. FoxP3 staining was performed with intracellular fixation/permeabilization protocol following manufacturer's recommendation (Biolegend). DAPI (4',6-diamidino-2-phenylindole), Ly6G (clone 1a8), CD11b (clone M1/70), Gr-1 (clone RB6-8C5), CXCR4 (clone 2B11), CD62L (clone MEL-14), CD16/32 (clone 93), MERTK (clone 2B10C42), Gr-1 (clone RB6-8C5), CD115 (clone AFS98), F4/80 (clone BM8), CXCR2 (clone SA044G4), VE-cadherin (clone BV13) NK-1.1 (clone PK136), CD3 (clone 17A2), FoxP3 (clone MF14), CD25 (clone 3C7) were purchased from Biolegend. Occludin (clone EPR20992) was purchased from Abcam.

### Blood counts

Total circulating blood leukocytes, neutrophils, lymphocyte, and monocytes were analyzed using the Hematrue Hematology Analyzer (Heska, Loveland CO).

### Neutrophil isolation, labeling and adoptive transfer

Neutrophils were isolated from bone marrow by negative selection (StemCell Technologies) with >90% purity. Fluorescence-activated cell sorting (FACS) was used to obtain naïve (DAPI<sup>-</sup>CD11b<sup>+</sup>Ly6G<sup>+</sup>CXCR4<sup>lo</sup>CD62L<sup>hi</sup>) and aged (DAPI<sup>-</sup>CD11b<sup>+</sup>Ly6G<sup>+</sup>CXCR4<sup>hi</sup>CD62L<sup>lo</sup>) neutrophils. Naïve neutrophils were obtained from blood or bone marrow, and aged neutrophils were obtained from blood.

Adoptive transfer was performed using neutrophils isolated from the bone marrow of GFP<sup>+</sup> mice. Recipient mice were injected intravenously with  $5 \times 10^6$  neutrophils. At the indicated times, blood and bone marrow were harvested. GFP<sup>+</sup> cells were gated by flow cytometry to determine their expression of CD62L and CXCR4 as a function of aging.

### Antibiotics and pharmacologic inhibitors

Mice were treated with ampicillin (1 g/L) streptomycin (1 g/L), metronidazole (1 g/L), and vancomycin (500 mg/L) in drinking water for 2 weeks before tumor inoculation or analysis of neutrophils and other cells. Drinking water containing antibiotics was changed twice per week. Control mice were fed normal drinking water, and both groups of mice were housed in the same animal facility and fed the same diet ad libitum.

Neutrophil elastase inhibition was performed by intraperitoneal (i.p.) injection (once daily for 3 d) of 50 mg/kg sivelestat (Tocris). MMP-9 inhibition was achieved by i.p. injections (once daily for 3 d) of 50 mg/kg of SB-3CT (Tocris). NET inhibition was achieved by i.p. injection (once daily for 3 d) of 50  $\mu$ g DNase-I. The regimen and doses are consistent with previously reported treatments.<sup>22</sup>

Losartan (LKT Laboratories, St. Paul, MN) and hydralazine (Sigma, St Louis, MO) were dosed as we have previously reported. Both medications were provided in drinking water and the doses have similar effects on blood pressure as we have previously reported.<sup>23,24</sup> Candesartan (Sigma) was administered at 1 mg/kg/day by intraperitoneal injection.

### **Reactive oxygen species measurements**

Purified neutrophils were incubated with 5  $\mu\text{M}$  of 5-(and-6)-chloromethyl-2',7'-dichlorodihydrofluorescein diacetate, acetyl ester (CM-H2DCFDA, Invitrogen) at 37°C for 15 min before analysis by flow cytometry.

### **Enzyme-linked immunosorbent assay (ELISA)**

Measurements of VEGF, MMP-9, and elastase was performed by ELISA following manufacturer's instructions (R&D Biosystems).

### **Elastase activity**

Neutrophil elastase (NE) activity was determined using N-methoxysuccinyl Ala-Ala-Pro-Val-*p*-nitroanilide (M4765, Sigma), a highly specific synthetic substrate for NE. Briefly, a 100  $\mu\text{L}$  sample was incubated with 0.1 M Tris-HCl buffer (pH 8.0) containing 0.5 M NaCl and 1 mmol/L substrate in a final volume of 1.0 ml at 37°C for 24 h. The amount of *p*-nitroanilide liberated from the substrate by NE was measured spectrophotometrically at 405 nm and calculated from a standard curve of *p*-nitroanilide (185310, Sigma). One unit of NE activity was defined as the quantity of enzyme that liberated 10 mol/L of *p*-nitroanilide in 24 h.

### **Neutrophil extracellular trap (NET) measurement**

Abundance of extracellular DNA, a surrogate of NETs, was quantified using the SYTOX green assay. Aged and naïve neutrophils obtained from metastatic tumor-bearing mice were plated onto a 96-well plate and treated as described. 5  $\mu\text{M}$  SYTOX green dye (Invitrogen, Carlsbad, CA) was added to each well and the fluorescence was read with filter settings at 485-nm excitation/525-nm emission using a Synergy H1 Microplate Reader and Gene5 software (Biotek, Winooski, VT). The fluorescence was read every 5 min for a total of 2 h at 37°C. The fluorescence of each treatment was measured in triplicate between 90 and 120 min of each experiment at the early plateau of fluorescence.

### **Neutrophil-endothelial cell co-culture**

The human umbilical endothelial vein endothelial cells (HUVEC) were cultured in complete medium with 10% FBS.  $1 \times 10^5$  cells were cultured with purified neutrophils at a ratio of 5:1. After 6 h, the culture plate was spun down and supernatant was harvested. Cells were washed with FACS buffer and stained for VE-cadherin and occludin-1 as a measure of vascular endothelial permeability using flow cytometry.

### **Thioglycolate-elicited peritoneal macrophage co-culture**

Four days after 2 ml intraperitoneal injection of 3% thioglycolate, peritoneal cells were harvested in HBSS (containing 1 M

HEPES, 0.05% BSA, 0.025%  $\text{NaHCO}_3$ , 1% Pen/Strep). Macrophages were isolated with Percoll gradients consisting of 36% Percoll (vol/vol) and 72% Percoll (vol/vol) in PBS and cultured in either normal media or tumor-conditioned media overnight. Macrophages were washed and stained for MERTK expression by flow cytometry.

### **Splenic isolation**

Spleens of mice were digested by mechanical dissociation. Cells were washed, RBCs were lysed with ACK lysis buffer and stained for FACS analysis as described above. Granulocytic MDSCs of metastatic tumor-bearing mice were identified as  $\text{CD11b}^+\text{Ly6G}^+\text{Ly6C}^-$  cells.

### **In vitro neutrophil aging assays**

Bone marrow purified neutrophils were stimulated for 3 h with G-CSF (100 ng/ml), GM-CSF (100 ng/ml), or angiotensin II (Ang II) (100  $\mu\text{M}$ ). Neutrophils were cultured in the presence or absence of losartan (1  $\mu\text{M}$ ) or candesartan (1  $\mu\text{M}$ ).

### **qPCR**

RNA was extracted using Qiagen RNeasy Mini Kit according to the manufacturer's instructions. qRT-PCR was performed using Power SYBR Green PCR Master Mix (Applied Biosystems). Plates were read with an ABI 7900 (Applied Biosystems). Amplifications were carried out with the following primers:  
Scl27a2; F: GGAACCACAGGTCTTCCAAA, R: TAAAGTAGCCCCAACCACGA  
Beta actin; F: GGCACCACACCTTCTACAATG, R: GGGGTGTTGAAGGTCTCAAAC

### **Scratch assay**

Tumor cells were seeded in 24-well plates and cultured with control media (DMEM with 10% FCS) or media obtained from a 4-h culture of FACS-sorted aged or naïve neutrophils. A 200  $\mu\text{l}$  pipette tip was used to create a scratch wound at the center of the culture dish, and the diameter of the wound was measured at 0, 16, and 24 h. Data is presented as percent wound closure by calculating the diameter of the scratch surface area at the indicated time points relative to the total wound diameter at time 0 h.

### **Proliferation assay**

4T1 cells  $3 \times 10^3$  were seeded in 96-well microtiter plates in a final volume of 100  $\mu\text{l}$ /well culture medium by mixing regular DMEM medium with aged or naïve neutrophil-conditioned DMEM medium with a 2:1 ratio. Cells were incubated for 0, 24, 48, and 72 h. Then, 10  $\mu\text{l}$  WST-1 cell proliferation reagent (Biovision) was added to each well followed by incubation for 30 minutes under standard culture conditions. After plates were shaken vigorously for 1 minute on an orbital shaker, absorbance at 450 nm was measured with a microtiter plate reader.

## Efferocytosis assay

Aged neutrophils were obtained from tumor-bearing mice and labeled with CellTracker Green CMFDA (5-Chloromethylfluorescein Diacetate) dye (Sigma). Tumor-conditioned or control macrophages were incubated with neutrophils in a 1:1 ratio. After 1 h, macrophages were washed three times in cold PBS. Uptake of labeled neutrophils was measured by flow cytometry, measured as F4/80+ FITC+ double-positive cells after intracellular permeabilization. Signals were subtracted from non-permeabilized cells as negative controls.

## Statistical analysis

All results are expressed as mean  $\pm$  SEM, unless otherwise stated. Graphpad Prism (Graphpad Software, La Jolla, CA) was used for statistical analysis. Comparisons between two groups were analyzed by unpaired Student's *t* test or by ANOVA for experiments with means from more than 2 subgroups, followed by Tukey posthoc test. A *P* value of  $<0.05$  was considered statistically significant.

## Results

### CXCR4<sup>hi</sup>CD62L<sup>lo</sup> aged neutrophils are increased in tumor-bearing mice and promote metastasis

Given the importance of granulocytic inflammation in cancer metastasis,<sup>2,25</sup> we sought to determine how cancer cells exploit other neutrophils besides MDSCs to promote metastasis. Granulocytic MDSCs (gMDSCs) only emerge from an aberrant but distinct trajectory point along granulocyte differentiation,<sup>8</sup> indicating that the normal neutrophil differentiation trajectory

is preserved in cancer-bearing mice. Mature neutrophils are naïve (CXCR4<sup>lo</sup>CD62L<sup>hi</sup>) or aged (CXCR4<sup>hi</sup>CD62L<sup>lo</sup>).<sup>13</sup> We focused on aged neutrophils because CXCR4 is not a defining marker or pathway in any of the MDSC subsets identified by recent analysis.<sup>8</sup> Using the same flow cytometric gating strategy for aged neutrophils as previously reported<sup>13,15,26</sup> (Figure 1(a)), we found increased proportions of CXCR4<sup>hi</sup>CD62L<sup>lo</sup> neutrophils in the blood, lung, and liver of 4T1 breast cancer-bearing mice when compared to tumor-free mice (WT) (Figure 1(b)). Notably, the proportions of CXCR4<sup>hi</sup>CD62L<sup>lo</sup> neutrophils were higher in tissues compared to blood in mice with or without tumor, in keeping with previous observation that aged neutrophils infiltrate tissues during homeostasis.<sup>26</sup> These CXCR4<sup>hi</sup>CD62L<sup>lo</sup> cells in cancer-bearing mice are similar to the aged neutrophils reported in normal physiology and in chronic inflammatory states, as they express low CXCR2 and high CD11b (Figure S1A).

We also examined differences between gMDSCs and aged neutrophils. Using intracellular staining, flow cytometric analysis revealed that the expression of *Rb1*, the master negative regulator of MDSCs,<sup>27,28</sup> is upregulated approximately 10-fold in these neutrophils compared to gMDSC (Figure S1B). Furthermore, *Scl27a2*, a fatty acid transporter protein 2 (FATP2) encoding gene which is upregulated in gMDSCs,<sup>29</sup> is reduced 3-fold in aged neutrophils as indicated by RT-PCR analysis (Figure S1C). We did not compare suppression of T cells because several studies have shown that mature neutrophils do possess MDSC-like immunosuppressive capacity.<sup>30</sup>

We found that other metastatic cancers, including B16F10 and B16LS9 melanoma but not the non-metastatic counterpart B16F0, also caused accumulation of CXCR4<sup>hi</sup>CD62L<sup>lo</sup> aged neutrophils in blood and tissues (Figure 1(c)). Collectively,

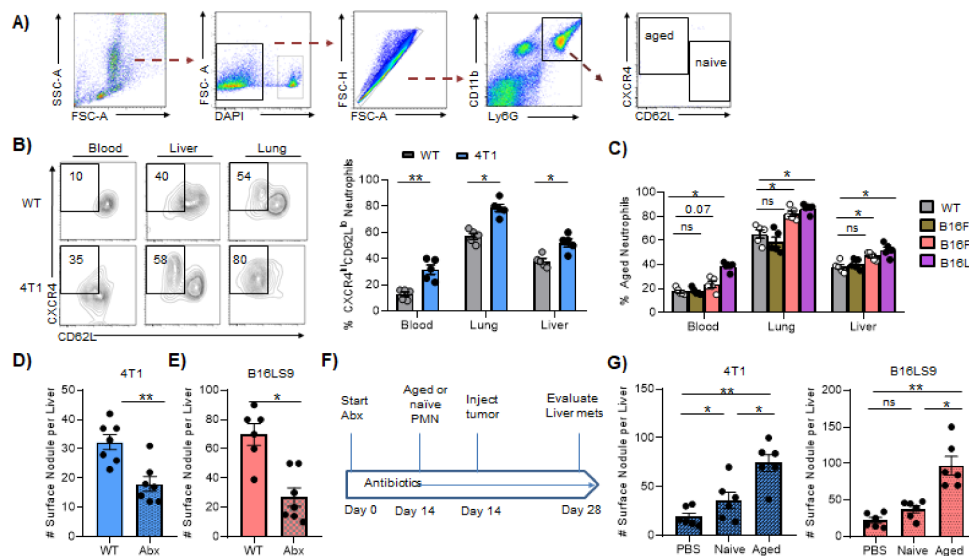


**Figure 1. CXCR4<sup>hi</sup>CD62L<sup>lo</sup> aged neutrophils accumulate in metastatic cancer.** (a) Gating strategy for the identification of CXCR4<sup>hi</sup>CD62L<sup>lo</sup> aged neutrophils in mice with or without metastatic tumor cells. (b) Flow cytometric assessment of CXCR4<sup>hi</sup>CD62L<sup>lo</sup> neutrophil proportions in blood, lung, and liver of WT (Balb/C) compared to mice inoculated with 4T1 for 14 d. *n* = 5 per group. (c) Proportions of aged neutrophil in blood, lung, and liver of WT (C57BL/6J) and mice inoculated with B16F10, B16F0, or B16LS9 tumor cells for 14 d. *n* = 5 per group. (d, e) Number of liver metastasis in mice treated with or without antibiotics. (d) shows 4T1 metastasis, while (e) indicates B16LS9 metastasis. Gut microbiota was depleted for 14 d before tumor inoculation. *n* = 7 per treatment group. (f) Strategy for treatment with antibiotic for 14 d to deplete aged neutrophils followed by i.v. adoptive transfer of naïve or aged neutrophils with tumor inoculation. (g) Number of liver metastasis by 4T1 (left) or B16LS9 (right) in antibiotic-treated mice receiving PBS, naïve or aged neutrophils. Data plotted as mean  $\pm$  SEM. Each symbol represents result from each mouse. ns = not significant, \**p* < .05, \*\**p* < .01 by *t* test except C,G (ANOVA).

these results indicate that metastatic cancers promote the accumulation of aged neutrophils.

We then examined the role of aged neutrophils in cancer metastasis by limiting their accumulation in an intrasplenic model of liver metastasis. Commercially available anti-Ly6G antibodies that are routinely used to deplete neutrophils target all granulocytes including MDSCs.<sup>31</sup> Moreover, CXCR4 inhibitors also nonspecifically target several cell types.<sup>32</sup> Thus, our approach to restrict *in vivo* CXCR4<sup>hi</sup>CD62L<sup>lo</sup> neutrophil accumulation was to use antibiotics to deplete the gut microbiome, which is known to regulate neutrophil aging.<sup>15</sup> As seen in Figure S2A-D, we confirmed that microbiome depletion did not alter the numbers of leukocytes in the circulation, except for neutrophils. Importantly, we confirmed that antibiotics reduced aged neutrophils not only in the blood as previously reported,<sup>15</sup> but also in the liver (Figure S2E,F). The microbiome-depleted mice showed reduced numbers of 4T1 and B16LS9 metastases in the liver (Figure 1(d,e)). For example, the number of liver 4T1 metastatic foci averaged  $32 \pm 2.6$ , compared to  $18 \pm 2.5$  for antibiotic-treated mice (Figure 1(d)). Of note, antibiotic use does not affect tumor cell viability (Figure S2G) or tumor cell proliferation (Figure S2H) *in vitro*.

Depleting the gut microbiome may have off-target effects. While the total splenic granulocytes were reduced after antibiotic treatment (Figure S2I), we found no differences in the proportions of other immunosuppressive cells that may influence metastasis, including natural killer (NK) cells (Figure S2J) and FoxP3+ regulatory T cells (Figure S2K). However, to definitively demonstrate that aged neutrophils are specifically responsible for the beneficial effects of gut microbiome depletion on liver metastatic growth, we

adoptively transferred either naïve or aged neutrophils from tumor-bearing mice into recipient microbiome-depleted mice before tumor inoculation (see schema in Figure 1(f)). Microbiome-depleted mice receiving aged neutrophils showed a far greater increase in liver metastatic deposits in both the 4T1 and B16LS9 models (Figure 1(g)), indicating that these cells are the predominant mediators of the observed reduction in metastasis. These results indicate that aged neutrophils play a crucial role in cancer metastasis to the liver.

### Metastatic cancers utilize multiple mechanisms to accumulate aged neutrophils

Next, we investigated the various mechanisms by which metastatic cancer cells cause accumulation of aged neutrophils in mice. Circulating aged neutrophils undergo a strict circadian fluctuation in numbers, reaching a peak during the day (ZT5) and a nadir after dark (ZT13).<sup>13</sup> Comparing WT (Balb/C) to intravenous 4T1-bearing mice, we found disruption in the circadian homeostasis of aged neutrophils. Specifically, WT showed predicted fluctuations in aged neutrophil numbers in the circulation, while the numbers showed no significant changes over time in 4T1 mice (Figure 2 (a)). Similar results were observed when comparing WT (C57BL6/J) to mice inoculated with B16LS9 melanoma cells, but not those inoculated with B16F0 cells, which possess an extremely low metastatic potential (Figure 2(b)).<sup>18</sup> These disruptions in homeostasis suggest enhanced tumor cell-induced neutrophil aging, impaired aged neutrophil clearance, or both. To assess tumor-induced enhanced aging, two approaches were used. First, we tested the possibility that tumor cells directly induce neutrophil aging. For

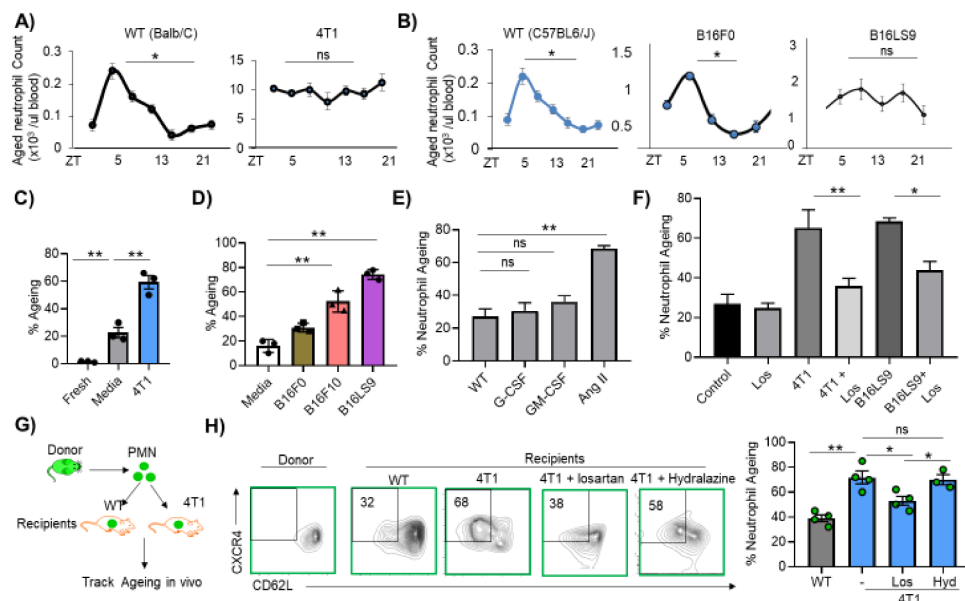


**Figure 2.** Metastatic cancers increase neutrophil aging. (a,b) Assessment of circadian fluctuations in CXCR4<sup>hi</sup>CD62L<sup>lo</sup> aged neutrophil numbers in the circulation at different times of the day (ZT0-ZT23). (a) represents BALB/c strain with or without syngeneic 4T1 tumor, and (b) shows  $n = 10$  per ZT time point per experimental group. (c,d) Analysis of *in vitro* neutrophil aging during co-culture of bone marrow neutrophils with control media or tumor-conditioned media. In (c), Balb/C cells are co-cultured with 4T1-conditioned media. In (d), C57BL6/J cells are co-cultured with control media or B16F0, B16F10, or B16LS9-conditioned media. Experiments were performed three independent times. (e) *In vitro* neutrophil aging by stimulation with G-CSF (100 ng/ml), GM-CSF (100 ng/ml), or angiotensin (Ang) II (100  $\mu$ M) for 3 h. (f) Effect of Ang II inhibition on neutrophil aging. Cells were treated with normal media or conditioned media from 4T1 or B16LS9 tumors. Experiments were performed for 3 hrs in the presence or absence of 1  $\mu$ M of losartan (Los). (g) Schema for the adoptive transfer of naïve neutrophils isolated from GFP mice into WT or 4T1-tumor-bearing mice. (h) Aging of the donor GFP cells were then assessed by flow cytometry. Recipient mice were untreated WT, or 4T1 mice with or without hydralazine or losartan.  $n = 3-4$  recipients per group. Each symbol represents result from one mouse. For cell cultures, cells from each mouse (three mice per experiment) were seeded in triplicates for each condition. Data plotted as mean  $\pm$  SEM. ns not significant,  $*p < .05$ ,  $**p < .01$  by ANOVA, except F (t test).

this, CXCR4<sup>lo</sup>CD62L<sup>hi</sup> naïve neutrophils from the bone marrow of Balb/C were FACS sorted and cultured *in vitro* with either control media or conditioned media from various tumors. 4T1-conditioned media robustly induced neutrophil aging compared to control media (59 ± 5% vs 22 ± 4%, **Figure 2(c)**). Similarly, B16F10 and B16LS9 tumor conditioned-media robustly induced aging in C57BL/6 WT neutrophils, whereas B16F0 cells induced neutrophil aging to a far less extent than its aggressive counterparts (31 ± 2% compared to 52 ± 5% by B16F10 and 81 ± 4% by B16LS9, **Figure 2(d)**).

We then determined the specific tumor-secreted factor(s) that drive neutrophil aging. Tumors influence granulopoiesis via increased production of G-CSF, GM-CSF, and angiotensin II (Ang II), among other factors.<sup>33,34</sup> *In vitro*, neither G-CSF nor GM-CSF significantly stimulated aging of naïve bone marrow isolated neutrophils. Instead, Ang II robustly induced neutrophil aging (**Figure 2(e)**). When neutrophils were pre-treated with losartan (an Ang II receptor blocker) before co-culture with tumor-conditioned media, neutrophil aging was diminished *in vitro* (**Figure 2(f)**). Thus, tumor cells directly promote neutrophil aging via Ang II.

The second approach we leveraged to investigate tumor-induced neutrophil aging was to adoptively transfer naïve GFP neutrophils into WT or 4T1 mice and track the fate of the donor GFP cells *ex vivo* (**Figure 2(g)**). If metastatic cancer indeed accelerates neutrophil aging, GFP+ cells identically injected into WT and 4T1 mice and isolated from these mice would show differential aging. Indeed, donor GFP neutrophils rapidly upregulated CXCR4 and downregulated CD62L in 4T1 mice when compared to WT (**Figure 2(h)**). In the same experimental design, two separate groups of 4T1-inoculated mice also received losartan (Los) or hydralazine (Hyd). The hydralazine group was included to account for any blood pressure changes that may be associated with losartan use. Treatment with losartan reduced neutrophil aging *in vivo* after adoptive transfer of GFP neutrophils, whereas hydralazine had no significant impact on aging of transferred cells in the metastatic cancer environment (**Figure 2(h)**). Similar results were obtained when GFP+ neutrophils were adoptively transferred into mice inoculated with B16LS9, where treatment with losartan also significantly reduced aging of donor cells (**Figure S3A**). To ensure that the losartan effect is not drug-specific, we used another Ang II receptor blocker, candesartan, to confirm angiotensin-induced neutrophil aging *in vitro* and *in vivo*. Similar to what was found in the losartan experiments, 4T1-bearing mice treated with candesartan showed reduced aging of adoptively transferred GFP neutrophils *in vivo* (**Figure S3B**). *In vitro*, candesartan also reduced neutrophil aging when cells are cultured in 4T1-conditioned media (**Figure S3C**). These studies confirm that the metastatic cancer environment accelerates neutrophil aging and that Ang II-increased in tumor-bearing mice<sup>33</sup> – mediates this effect.

We also investigated the known mechanisms associated with the clearance of aged neutrophils. It has been shown that aged neutrophils are removed at designated sites (predominantly liver and bone marrow) by efferocytic macrophages through liver X receptor target genes such as *Mertk*.<sup>13,35</sup> However, MERTK protein expression on the macrophage cell surface may be cleaved in the setting of

chronic inflammation, thereby reducing their ability to efferocytose neutrophils.<sup>36,37</sup> Thus, we examined macrophage MERTK expression in the presence or absence of tumor-conditioned media using flow cytometry. Interestingly, macrophages cultured with tumor-conditioned media showed 50% increased shedding of MERTK (**Figure S4A**). However, the uptake of aged neutrophils by macrophages exposed to tumor-conditioned media was not significantly different from those conditioned with normal media. For instance, 1 hr after co-culture with aged neutrophils, tumor-conditioned macrophages showed efferocytosis of approximately 27.8 ± 3.2%, compared to 25% ± 2 uptake by control macrophages (**Figure S4B**). *In vivo*, bone marrow efferocytic macrophage numbers were lower in 4T1 and B16LS9-inoculated mice when compared to their syngeneic control WT (**Figure S4C**). However, the expression of MERTK on bone marrow macrophages in mice inoculated with either 4T1 or B16LS9 tumor cells was unchanged when compared to their syngeneic controls (**Figure S4D**). Thus, although the number of aged neutrophils is increased in metastatic tumor-inoculated mice, there is no increase in the number of efferocytic macrophages in these mice *in vivo*, suggesting an inadequate compensatory mechanism. Thus, metastatic tumors promote accumulation of aged neutrophils in part via direct stimulation of neutrophil aging, disruption of the circadian neutrophil homeostasis, and failure to adequately enhance efferocytic clearance of aged neutrophils.

### **Aged neutrophils have enhanced metastasis-inducing features**

Next, we sought to determine the functional properties of aged neutrophils to assess their role in supporting metastasis. We focused on neutrophil functions associated with metastasis, such as reactive oxygen species (ROS) production, neutrophil extracellular trap (NETs) release, and metalloprotease release.<sup>25</sup> Aged neutrophils from both B16LS9 and 4T1 mice produced significantly more NETs (1.5-fold) than their naïve counterparts as measured by sytox green fluorescence (**Figure 3(a)**). ROS production was also markedly elevated in aged neutrophils (1.5-fold) as measured by the cell-permeant 2',7'-dichlorodihydrofluorescein diacetate (H2-DCFDA) assay (**Figure 3(b)**). Aged neutrophils released far more MMP-9 (2.3-fold **Figure 3(c)**) and had greater neutrophil elastase activity (4.5-fold, **Figure 3(d)**). Because neutrophils can also directly interact with endothelial cells to promote metastasis, aged and naïve neutrophils were co-cultured with endothelial cell line HUVEC. The expression of occludin and VE-cadherin, two markers of endothelial barrier integrity,<sup>38</sup> was assessed by flow cytometry. These experiments revealed suppressed occludin and VE-cadherin expression in the presence of aged neutrophils when compared to naïve neutrophils (**Figure 3(e,f)**). Finally, in a prototypical wound-closure assay to assess migration, tumor cells conditioned with media from aged neutrophils rapidly migrated and covered the entire scratch area by 24 h (**Figure 3(g)**). There was no difference in tumor cell proliferation when co-cultured with naïve or aged neutrophils (**Figure 3(h)**). These data indicate that aged neutrophils are endowed with a variety of features that promote cancer metastasis.

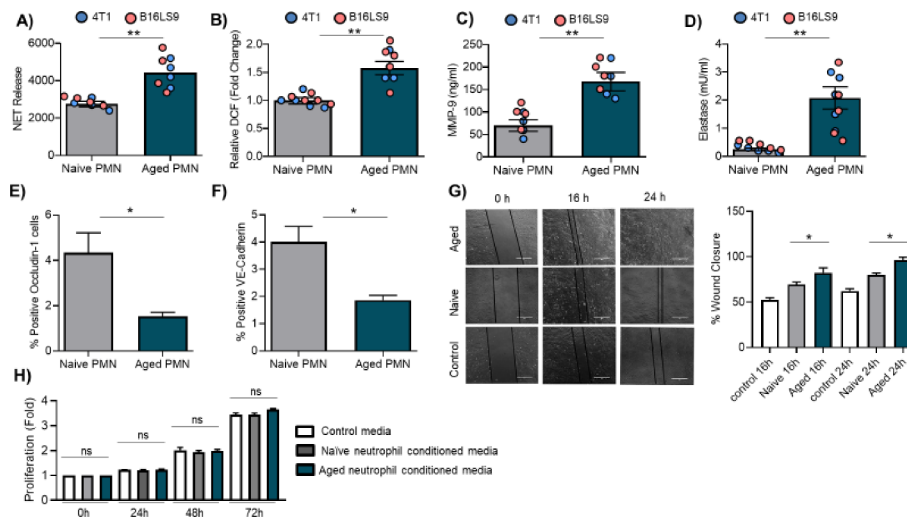


**Figure 3.** Characteristics of aged neutrophils. Measurement of (a) neutrophil extracellular traps (NETs), (b) ROS, (c) matrix-metalloproteinase 9 (MMP-9), and (d) neutrophil elastase from naïve and aged neutrophils obtained from 4T1 (blue) and B16F10 (pink) tumor-bearing mice.  $n = 4-5$  mice per tumor condition. Flow cytometric assessment of the expression of occludin-1 (e) and VE-cadherin (f) by HUVEC cells cultured in the presence of naïve or aged neutrophils. (g) Representative images and quantitation of migration of tumor cells over a scratch wound at 0, 16, and 24 h. Tumor cells (4T1) were cultured with control media, naïve neutrophil media, or aged neutrophil media. Experiment was performed two independent times. (h) Measurement of tumor proliferation during co-culture with normal media or media conditioned from aged or naïve neutrophils. Cells were cultured up to 72 h. NS not significant,  $*p < .05$ ,  $**p < .01$  by unpaired Student's  $t$  test. Data are plotted as mean  $\pm$  SEM.

Finally, we evaluated the *in vivo* mechanisms by which aged neutrophils promote metastasis to the liver. Our approach was to inoculate mice with tumor, adoptively transfer aged neutrophils, and treat with either SB-3CT (MMP-9 inhibitor), sivelestat (elastase inhibitor), or DNase I (NETs inhibitor). After intrasplenic inoculation with either B16LS9 or 4T1 cancer cells (see Figure 4(a) for schema). Inhibitor treatment was

performed for only 3 d and stopped in order to restrict their effects to the factors released by the adoptively transferred aged neutrophils. Fourteen days after tumor cell injection, 4T1 surface nodules in the liver were significantly reduced by MMP-9 blockade, elastase blockade, or NET inhibition (Figure 4(b)). However, NET blockade achieved the greatest tumor reduction. In this 4T1 model, MMP-9 inhibition did not completely

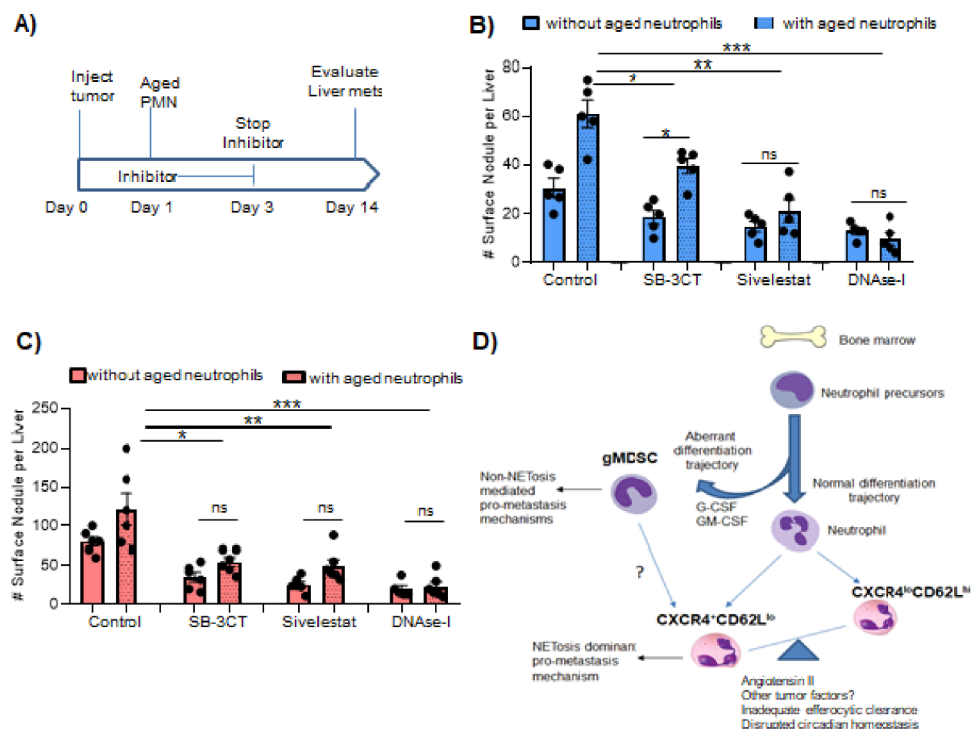


**Figure 4.** CXCR4<sup>hi</sup>CD62L<sup>lo</sup> aged neutrophils promote tumor metastasis via NETs. (a) Experimental design for the transfer of aged neutrophils and treatment with specific inhibitors after tumor inoculation. (b) Effect of MMP9 inhibitor (sivelestat, 50 mg/kg), neutrophil elastase inhibitor (SB-3 CT, 50 mg/kg) and NETs inhibitor (DNase I, 50  $\mu$ g) on 4T1 tumor metastasis to the liver.  $n = 5$  mice per treatment group. (c) Effect of sivelestat (50 mg/kg), SB-3 CT (50 mg/kg), and DNase I (50  $\mu$ g) on B16LS9 metastasis to the liver.  $n = 6$  mice per treatment group. ns = not significant.  $*p < .05$ ,  $**p < .01$ ,  $***p < .001$  by Tukey test. Data are plotted as mean  $\pm$  SEM. (d) Proposed mechanism for diversified approaches used by cancer cells to utilize granulocytes to promote metastasis.

abrogate the effect of aged neutrophil transfer, whereas NET blockade dramatically reduced metastasis with or without adoptive neutrophil transfer (Figure 4(b)). Similarly, as shown in Figure 4(c), NET inhibition showed the greatest reduction in liver metastasis when aged neutrophils were adoptively transferred in the B16LS9 model. We note, here again, that either MMP-9 or NET inhibition significantly reduced metastasis after aged neutrophil transfer. These results demonstrate that NETs play a dominant role in the effects of aged neutrophils on tumor metastasis.

## Discussion

To promote inflammation, metastatic cancers cause increased granulopoiesis and the expansion of immature cells from aberrant differentiation of myeloid lineage cells.<sup>2,7</sup> This is exemplified by the expansion of myeloid-derived suppressor cells (MDSCs) from a novel differentiation trajectory, which is particularly prominent in the spleen.<sup>8</sup> The central finding of our work is that metastatic cancers also markedly expand the proportion of CXCR4<sup>hi</sup>CD62L<sup>lo</sup> mature aged neutrophils. Whereas GM-CSF and G-CSF have been shown to mediate the expansion of MDSCs, here we found Ang II to be the critical player that robustly contributed to neutrophil aging. Aged neutrophils appear to be distinct from granulocytic MDSCs in that their expression profile of *Rb1* and *Sc127a2*, two transcriptional regulators of MDSCs, is distinct from MDSCs.<sup>28,29</sup> Moreover, CXCR4 expression is not a defining marker for MDSCs.<sup>8</sup>

Compared to their CXCR4<sup>lo</sup>CD62L<sup>hi</sup> naïve counterparts, aged neutrophils are greater contributors to liver metastasis in models of breast cancer and melanoma. Aged neutrophils possess several features, such as excessive production of neutrophil extracellular traps, reactive oxygen species, and MMP9, all previously shown to promote metastasis. Inhibition of NET formation by elastase or DNase-I treatment had the most prominent effect in ameliorating the metastasis-promoting effects of aged neutrophils. Multiple mechanisms have been proposed by which NETs promote cancer metastasis, including proteolytic remodeling of microenvironment that favors tumor cell adhesion, proliferation, migration, and invasion.<sup>22,39,40</sup> NETs have also been shown to physically shield tumor cells and thereby protect them from T cell- or natural killer (NK) cell-mediated toxicity.<sup>41</sup> Thus, the preferentially increased NET production by aged neutrophils is in accordance with their capacity to promote cancer metastasis.

Whether the CXCR4<sup>hi</sup>CD62L<sup>lo</sup> aged neutrophils in tumor-bearing mice are identical to the aged neutrophils that occur in normal homeostasis is unclear at this time. Aged neutrophils in homeostasis represent a highly activated neutrophil subset that are also increased in other chronic inflammatory models, including sickle cell disease.<sup>15</sup> Moreover, they express several tumor-promoting factors, including NETs and Mac-1, both of which have been shown to enhance successful metastatic seeding in the liver.<sup>17</sup> Thus, the CXCR4<sup>hi</sup>CD62L<sup>lo</sup> cells that accumulate in metastatic tumor-bearing mice and those that occur

in normal physiology are likely identical in some features. Of note, when we used antibiotics to deplete the microbiome to indirectly reduce aged neutrophil numbers before tumor inoculation – a condition that mimics regulation of physiologic-aged neutrophils rather than tumor-induced aging – metastasis was reduced. These data suggest the physiologic-aged neutrophils also favor metastasis and may be identical with those that emerge solely after tumor inoculation. Indeed, previous transcriptional analysis of aged neutrophils also showed that they share similar features with TNF-activated neutrophils, although other distinct pathways were not uniformly shared between activated and aged neutrophils.<sup>15</sup> Thus, further work is required to more clearly delineate the influence of tumor-associated inflammation and other sources on inflammation on neutrophil aging.

Another unresolved issue pertains to the interrelationship between CXCR4<sup>hi</sup>CD62L<sup>lo</sup> aged neutrophils and tumor-associated neutrophils (TAN). Indeed, the identity and origins of TAN remain incompletely understood but are more associated with primary tumor microenvironment.<sup>42</sup> On one hand, splenectomy reduces the number of TAN in multiple models, suggesting that the emergence of TANs is dependent on MDSCs.<sup>4</sup> On the other hand, the tumor environment directly polarizes and reactivates infiltrating neutrophils presumably recruited from the blood circulation.<sup>43</sup> As we demonstrated here, the metastasis environment also induces neutrophil aging. Therefore, it is possible that CXCR4<sup>hi</sup>CD62L<sup>lo</sup> aged neutrophils contribute to the so-called N2 TAN population and vice versa. However, this assumption is merely speculative, because although N2 TANs promote primary tumor growth, CD16<sup>high</sup>CD62L<sup>dim</sup> neutrophils that infiltrate human primary tumor site were found to be associated with better survival.<sup>44</sup> In that study, the role of these cells in metastasis was not ascertained. Notably, these cells express high CD11b, CD18, and NETs, which makes them similar to aged neutrophils. Extensive work is required to distinguish between the role of aged neutrophils in primary tumor growth compared to metastatic growth, as well as to characterize their relationship with other TANs.

In summary, our work shows that CXCR4<sup>hi</sup>CD62L<sup>lo</sup> aged neutrophils are the dominant mature neutrophil subset that drive inflammation and promote metastasis.

We propose that, to maximize neutrophilic inflammation, metastatic cancers use distinct multi-pronged approaches: one that focuses on granulocyte production arm to generate MDSCs, and another that exploits the clearance/homeostasis arm to accumulate mature-aged neutrophils. These two populations use specific modalities to support the inflammation that drives metastasis (Figure 4(d)). Notably, NET formation, which appears to be a dominant mechanism by which aged neutrophils promote metastasis, is not a major feature by which MDSCs promote metastasis.<sup>7</sup> Although both melanoma and breast cancer models we investigated exploited aged neutrophils, distinct cancer types and distinct stages of the metastatic process may differentially rely on MDSCs, aged neutrophils, or both, to facilitate metastasis. Targeting aged neutrophils may serve as an attractive yet unexplored means

to inhibit cancer metastasis.

## Acknowledgments

This work was supported by NIH R01AI134714 (KEB), K99 HL141638 (DOD), R01 HL142677 (JFG), 2R01CA151610, Department of Defense (W81XWH-18-1-0067), the Fashion Footwear Charitable Foundation of New York, Inc, and the Margie and Robert E. Petersen Foundation (XC), and a seed grant from the Department of Pathology, Cedars-Sinai Medical Center.

## Disclosure of potential conflicts of interest

Authors declare no conflict of interest.

## Funding

This work was supported by the National Heart, Lung, and Blood Institute [HL142677]; National Heart, Lung, and Blood Institute [HL141638]; National Institute of Allergy and Infectious Diseases [R01AI134714]; U.S. Department of Defense [W81XWH-18-1-0067]; National Cancer Institute [R01CA151610].

## ORCID

Derick Okwan-Duodu  <http://orcid.org/0000-0003-1479-5759>

## Author contributions

Conceptualization: DOD, XC, KEB  
 Experimental Design: DOD, XC  
 Experiments: ZP, CL, DYC, LCV, EAB, DOD  
 Analysis & Interpretation: DOD, XC, ZP  
 Writing (original draft): ZP, DOD, XC;  
 Writing (review and editing): all authors  
 Resources: DOD, KEB, XC.

## References

- Chaffer CL, Weinberg RA. A perspective on cancer cell metastasis. *Science*. 2011;331(6024):1559–1564. doi:10.1126/science.1203543.
- Coussens LM, Werb Z. Inflammation and cancer. *Nature*. 2002;420(6917):860–867. doi:10.1038/nature01322.
- Grivennikov SI, Greten FR, Karin M. Immunity, inflammation, and cancer. *Cell*. 2010;140(6):883–899. doi:10.1016/j.cell.2010.01.025.
- Cortez-Retamozo V, Etzrodt M, Newton A, Rauch PJ, Chudnovskiy A, Berger C, Ryan RJH, Iwamoto Y, Marinelli B, Gorbato R, et al. Origins of tumor-associated macrophages and neutrophils. *Proc Natl Acad Sci U S A*. 2012;109(7):2491–2496. doi:10.1073/pnas.1113744109.
- Mantovani A, Allavena P, Sica A, Balkwill F. Cancer-related inflammation. *Nature*. 2008;454(7203):436–444. doi:10.1038/nature07205.
- Templeton AJ, McNamara MG, Seruga B, Vera-Badillo FE, Aneja P, Ocana A, Leibowitz-Amit R, Sonpavde G, Knox JJ, Tran B, et al. Prognostic role of neutrophil-to-lymphocyte ratio in solid tumors: a systematic review and meta-analysis. *J Natl Cancer Inst*. 2014;106(6):dju124. doi:10.1093/jnci/dju124.
- Kumar V, Patel S, Tcyganov E, Gabrilovich DI. The nature of myeloid-derived suppressor cells in the tumor microenvironment. *Trends Immunol*. 2016;37(3):208–220. doi:10.1016/j.it.2016.01.004.
- Alshetaiwi H, Pervolarakis N, McIntyre LL, Ma D, Nguyen Q, Rath JA, Nee K, Hernandez G, Evans K, Torosian L, et al. Defining the emergence of myeloid-derived suppressor cells in breast cancer using single-cell transcriptomics. *Sci Immunol*. 2020;5(44):eaay6017. doi:10.1126/sciimmunol.aay6017.
- Granot Z, Henke E, Comen EA, King TA, Norton L, Benezra R. Tumor entrained neutrophils inhibit seeding in the premetastatic lung. *Cancer Cell*. 2011;20(3):300–314. doi:10.1016/j.ccr.2011.08.012.
- Lopez-Lago MA, Posner S, Thodima VJ, Molina AM, Motzer RJ, Chaganti RS. Neutrophil chemokines secreted by tumor cells mount a lung antimetastatic response during renal cell carcinoma progression. *Oncogene*. 2013;32(14):1752–1760. doi:10.1038/onc.2012.201.
- Ng LG, Ostuni R, Hidalgo A. Heterogeneity of neutrophils. *Nat Rev Immunol*. 2019;19(4):255–265. doi:10.1038/s41577-019-0141-8.
- Adrover JM, Del Fresno C, Crainiciuc G, Cuartero MI, Casanova-Acebes M, Weiss LA, Huerga-Encabo H, Silvestre-Roig C, Rossaint J, Cossío I, et al. A neutrophil timer coordinates immune defense and vascular protection. *Immunity*. 2019;50(2):390–402 e10. doi:10.1016/j.immuni.2019.01.002.
- Casanova-Acebes M, Pitaval C, Weiss LA, Nombela-Arrieta C, Chevre R, AG N, Kunisaki Y, Zhang D, van Rooijen N, Silberstein L, et al. Rhythmic modulation of the hematopoietic niche through neutrophil clearance. *Cell*. 2013;153(5):1025–1035. doi:10.1016/j.cell.2013.04.040.
- Uhl B, Vadlau Y, Zuchtriegel G, Nekolla K, Sharaf K, Gaertner F, Massberg S, Krombach F, Reichel CA. Aged neutrophils contribute to the first line of defense in the acute inflammatory response. *Blood*. 2016;128(19):2327–2337. doi:10.1182/blood-2016-05-718999.
- Zhang D, Chen G, Manwani D, Mortha A, Xu C, Faith JJ, Burk RD, Kunisaki Y, Jang J-E, Scheiermann C, et al. Neutrophil ageing is regulated by the microbiome. *Nature*. 2015;525(7570):528–532. doi:10.1038/nature15367.
- Zhang DC, Frenette PS. Cross talk between neutrophils and the microbiota. *Blood*. 2019;133(20):2168–2177. doi:10.1182/blood-2018-11-844555.
- Spicer JD, McDonald B, Cools-Lartigue JJ, Chow SC, Giannias B, Kubes P, Ferri LE. Neutrophils promote liver metastasis via Mac-1-mediated interactions with circulating tumor cells. *Cancer Res*. 2012;72(16):3919–3927. doi:10.1158/0008-5472.CAN-11-2393.
- Fidler IJ. Selection of successive tumour lines for metastasis. *Nat New Biol*. 1973;242(118):148–149. doi:10.1038/newbio242148a0.
- Shen XZ, Li P, Weiss D, Fuchs S, Xiao HD, Adams JA, Williams IR, Capecchi MR, Taylor WR, Bernstein KE, et al. Mice with enhanced macrophage angiotensin-converting enzyme are resistant to melanoma. *Am J Pathol*. 2007;170(6):2122–2134. doi:10.2353/ajpath.2007.061205.
- Evrard M, Kwok IWH, Chong SZ, Teng KWW, Becht E, Chen J, Siow JL, Penny HL, Ching GC, Devi S, et al. Developmental analysis of bone marrow neutrophils reveals populations specialized in expansion, trafficking, and effector functions. *Immunity*. 2018;48(2):364–79 e8. doi:10.1016/j.immuni.2018.02.002.
- Chow A, Lucas D, Hidalgo A, Mendez-Ferrer S, Hashimoto D, Scheiermann C, Battista M, Leboeuf M, Prophete C, van Rooijen N, et al. Bone marrow CD169+ macrophages promote the retention of hematopoietic stem and progenitor cells in the mesenchymal stem cell niche. *J Exp Med*. 2011;208(2):261–271. doi:10.1084/jem.20101688.
- Albregues J, Shields MA, Ng D, Park CG, Ambrico A, Poindexter ME, Upadhyay P, Uyeminami DL, Pommier A, Küttner V, et al. Neutrophil extracellular traps produced during inflammation awaken dormant cancer cells in mice. *Science*. 2018;361(6409):eaao4227. doi:10.1126/science.aao4227.
- Cao DY, Spivia WR, Veiras LC, Khan Z, Peng Z, Jones AE, Bernstein EA, Saito S, Okwan-Duodu D, Parker SJ, et al. ACE overexpression in myeloid cells increases oxidative metabolism and cellular ATP. *J Biol Chem*. 2020;295(5):1369–1384. doi:10.1074/jbc.RA119.011244.

24. Bernstein KE, Koronyo Y, Salumbides BC, Sheyn J, Pelissier L, Lopes DH, Shah KH, Bernstein EA, Fuchs D-T, Yu JY, et al. Angiotensin-converting enzyme overexpression in myelomonocytes prevents Alzheimer's-like cognitive decline. *J Clin Invest.* 2014;124(3):1000–1012. doi:10.1172/JCI66541.
25. Coffelt SB, Wellenstein MD, de Visser KE. Neutrophils in cancer: neutral no more. *Nat Rev Cancer.* 2016;16(7):431–446. doi:10.1038/nrc.2016.52.
26. Kim JH, Podstawka J, Lou Y, Li L, Lee EKS, Divangahi M, Petri B, Jirik FR, Kelly MM, Yipp BG, et al. Aged polymorphonuclear leukocytes cause fibrotic interstitial lung disease in the absence of regulation by B cells. *Nat Immunol.* 2018;19(2):192–201. doi:10.1038/s41590-017-0030-x.
27. Mastio J, Condamine T, Dominguez G, Kossenkov AV, Donthireddy L, Veglia F, Lin C, Wang F, Fu S, Zhou J, et al. Identification of monocyte-like precursors of granulocytes in cancer as a mechanism for accumulation of PMN-MDSCs. *J Exp Med.* 2019;216(9):2150–2169. doi:10.1084/jem.20181952.
28. Youn JI, Gabrilovich DI. New roles of Rb1 in expansion of MDSCs in cancer. *Cell Cycle.* 2013;12(9):1329–1330. doi:10.4161/cc.24577.
29. Veglia F, Tyurin VA, Blasi M, De Leo A, Kossenkov AV, Donthireddy L, To TKJ, Schug Z, Basu S, Wang F, et al. Fatty acid transport protein 2 reprograms neutrophils in cancer. *Nature.* 2019;569(7754):73–78. doi:10.1038/s41586-019-1118-2.
30. Aarts CEM, Hiemstra IH, Beguin EP, Hoogendijk AJ, Bouchmal S, van Houdt M, Tool ATJ, Mul E, Jansen MH, Janssen H, et al. Activated neutrophils exert myeloid-derived suppressor cell activity damaging T cells beyond repair. *Blood Adv.* 2019;3(22):3562–3574. doi:10.1182/bloodadvances.2019031609.
31. Finisguerra V, Di Conza G, Di Matteo M, Serneels J, Costa S, Thompson AA, Wauters E, Walmsley S, Prenen H, Granot Z, et al. MET is required for the recruitment of anti-tumoural neutrophils. *Nature.* 2015;522(7556):349–353. doi:10.1038/nature14407.
32. Debnath B, Xu S, Grande F, Garofalo A, Neamati N. Small molecule inhibitors of CXCR4. *Theranostics.* 2013;3(1):47–75. doi:10.7150/thno.5376.
33. Cortez-Retamozo V, Etzrodt M, Newton A, Ryan R, Pucci F, Sio SW, Kuswanto W, Rauch P, Chudnovskiy A, Iwamoto Y, et al. Angiotensin II drives the production of tumor-promoting macrophages. *Immunity.* 2013;38(2):296–308. doi:10.1016/j.immuni.2012.10.015.
34. Casbon AJ, Reynaud D, Park C, Khuc E, Gan DD, Schepers K, Passegué E, Werb Z. Invasive breast cancer reprograms early myeloid differentiation in the bone marrow to generate immunosuppressive neutrophils. *Proc Natl Acad Sci U S A.* 2015;112(6):E566–75. doi:10.1073/pnas.1424927112.
35. Hong C, Kidani Y, Noelia A, Phung T, Ito A, Rong X, Ericson K, Mikkola H, Beaven SW, Miller LS, et al. Coordinate regulation of neutrophil homeostasis by liver X receptors in mice. *J Clin Invest.* 2012;122(1):337–347. doi:10.1172/JCI58393.
36. Cai B, Kasikara C, Doran AC, Ramakrishnan R, Birge RB, Tabas I. MerTK signaling in macrophages promotes the synthesis of inflammation resolution mediators by suppressing CaMKII activity. *Sci Signal.* 2018;11(549):eaar3721. doi:10.1126/scisignal.aar3721.
37. Thorp E, Vaisar T, Subramanian M, Mautner L, Blobel C, Tabas I. Shedding of the Mer tyrosine kinase receptor is mediated by ADAM17 protein through a pathway involving reactive oxygen species, protein kinase Cdelta, and p38 mitogen-activated protein kinase (MAPK). *J Biol Chem.* 2011;286(38):33335–33344. doi:10.1074/jbc.M111.263020.
38. Gavard J, Gutkind JS. VE-cadherin and claudin-5: it takes two to tango. *Nat Cell Biol.* 2008;10(8):883–885. doi:10.1038/ncb0808-883.
39. Tohme S, Yazdani HO, Al-Khafaji AB, Chidi AP, Loughran P, Mowen K, Wang Y, Simmons RL, Huang H, Tsung A, et al. Neutrophil extracellular traps promote the development and progression of liver metastases after surgical stress. *Cancer Res.* 2016;76(6):1367–1380. doi:10.1158/0008-5472.CAN-15-1591.
40. Rayes RF, Mouhanna JG, Nicolau I, Bourdeau F, Giannias B, Rousseau S, Quail D, Walsh L, Sangwan V, Bertos N, et al. Primary tumors induce neutrophil extracellular traps with targetable metastasis promoting effects. *JCI Insight.* 2019;5. doi:10.1172/jci.insight.128008
41. Teijeira A, Garasa S, Gato M, Alfaro C, Migueliz I, Cirella A, de Andrea C, Ochoa MC, Otano I, Etxeberria I, et al. CXCR1 and CXCR2 chemokine receptor agonists produced by tumors induce neutrophil extracellular traps that interfere with immune cytotoxicity. *Immunity.* 2020;52(5):856–71 e8. doi:10.1016/j.immuni.2020.03.001.
42. Fridlender ZG, Albelda SM. Tumor-associated neutrophils: friend or foe? *Carcinogenesis.* 2012;33(5):949–955. doi:10.1093/carcin/bgs123.
43. Fridlender ZG, Sun J, Kim S, Kapoor V, Cheng G, Ling L, Worthen GS, Albelda SM. Polarization of tumor-associated neutrophil phenotype by TGF-beta: “N1” versus “N2” TAN. *Cancer Cell.* 2009;16(3):183–194. doi:10.1016/j.ccr.2009.06.017.
44. Millrud CR, Kagedal A, Kumlien Georen S, Winqvist O, Uddman R, Razavi R, Munck-Wikland E, Cardell LO. NET-producing CD16 high CD62L dim neutrophils migrate to tumor sites and predict improved survival in patients with HNSCC. *Int J Cancer.* 2017;140(11):2557–2567. doi:10.1002/ijc.30671.